

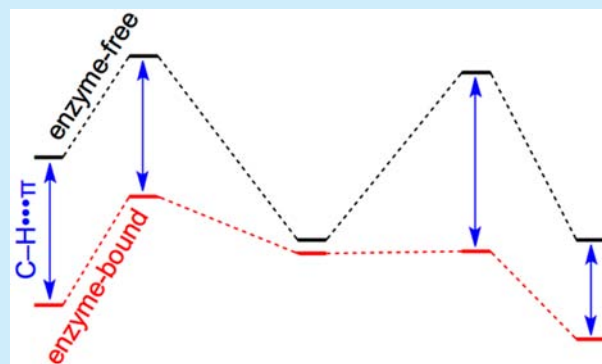
Tension between Internal and External Modes of Stabilization in Carbocations Relevant to Terpene Biosynthesis: Modulating Minima Depth via C–H $\cdots\pi$ Interactions

Young J. Hong and Dean J. Tantillo*

Department of Chemistry, University of California—Davis, Davis, California 95616, United States

S Supporting Information

ABSTRACT: Density functional theory calculations on a carbocation rearrangement relevant to the biosynthesis of the sesquiterpenoid trefolane A are described, with a focus on the viability of altering the curvature of the potential energy surface through C–H $\cdots\pi$ interactions of the sort likely to be found at the active site of a terpene synthase enzyme. These interactions are able to remove a deep minimum from a pathway to product.



How can a reacting molecule avoid becoming trapped in a deep minimum on a potential energy surface, when such a minimum exists along the reaction coordinate to products? This question is relevant to all branches of chemistry.¹ Here we describe an example of how a deep minimum can be converted to a shallow minimum by judiciously placed C–H $\cdots\pi$ interactions.²

During the course of our studies on carbocation cyclization/rearrangement reactions that form terpene natural products,³ we encountered a variety of reaction coordinates where deep minima impeded progress toward terpene products.⁴ While most terpene-forming pathways do not involve deep minima, allowing inherent carbocation reactivity to be expressed inside active site cavities,^{3,5,6} a small percentage do. Given the huge number of terpenes formed in nature (thousands of carbon skeletons, tens of thousands of functionalized derivatives),⁷ even a problem faced by a small fraction of terpene-forming reactions is itself far-reaching. We previously described one strategy for avoiding this problem for the case of trichodiene (1, Figure 1) formation; a competing mechanism, i.e., a different reaction coordinate/pathway to product, can be followed to avoid a deep minimum.⁶ We also suggested that nonstatistical dynamics effects⁸ might result in trajectories that avoid deep minima for terpene-forming carbocation reactions,⁴ a contention with some support in studies on smaller systems.^{1a,9} Furthermore, we showed previously that C–H $\cdots\pi$ and C–H \cdots lone pair interactions can modulate carbocation structures,¹⁰ as suggested in seminal work by Jensen and Jorgensen,¹¹ and that C–H \cdots lone pair interactions can alter the lifetimes of carbocations (as assessed via dynamics trajectory calculations).¹² In an effort to see whether such ostensibly weak interactions might also be capable of modulating the curvature of potential energy surfaces such that deep minima are rendered shallow, opening up another solution to the deep

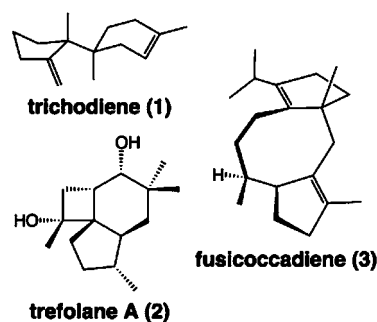


Figure 1. Structures of trichodiene (1), trefolane A (2), and fusicoccadiene (3).

minimum problem, we examined complexes of benzene, water, and/or ammonia with carbocations along the reaction coordinates for formation of trichodiene (1),⁶ trefolane A (2),¹³ and fusicoccadiene (3),¹⁴ systems known to have deep minima along reaction coordinates to terpene products (Figure 1). So far, we have found one case, a carbocation rearrangement en route to trefolane A (2) with a benzene molecule bound to species along the reaction coordinate in a particular orientation, where a reaction coordinate was so modulated.¹⁵

The example described here highlights the potential of carbocation– π interactions in terpene synthase active sites to promote product formation through direct intervention. Although others have described examples of mutations of aromatic residues in terpene synthase active sites that lead to

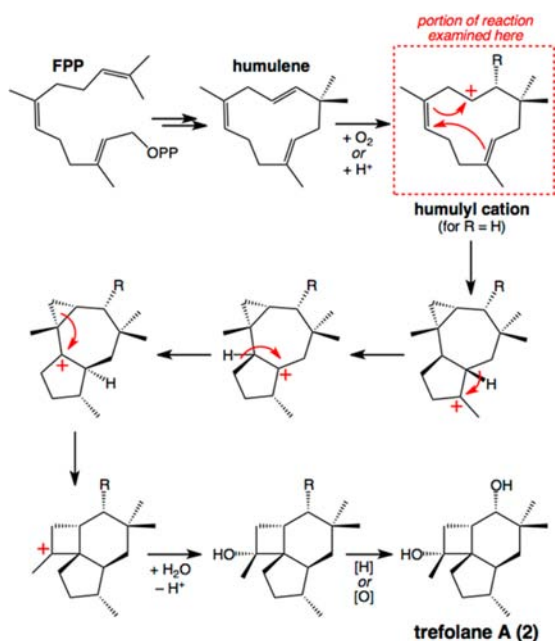
Received: September 21, 2015

Published: October 27, 2015

altered activity,¹⁶ and combined quantum mechanics/molecular mechanics (QM/MM) and automated docking studies have provided insight into the influence of factors such as shape selection in promoting cyclizations/rearrangements,^{3,17} the results described here reveal the magnitude of changes to reaction coordinate curvature that can be achieved via carbocation–active site association.

Two putative reaction mechanisms for formation of trefolane A (2) are shown in Scheme 1: one proposed in the original report

Scheme 1. Putative Mechanisms for Formation of Trefolane A^a



^aFPP = farnesyl diphosphate, OPP = pyrophosphate.

on its isolation (R = O–O[−]),¹³ and a variation involving formation of trefolane A's carbon skeleton prior to oxidation (R

= H; this second mechanism can also be formulated without the intermediacy of humulene). We subjected the latter to density functional theory (DFT) calculations at several levels of theory (in the absence of an enzyme).¹⁸ Structures from M06-2X/6-31+G(d,p) calculations are shown in Figure 2; only structures from the portion of the reaction coordinate where a deep minimum is found (with barriers in both the forward and reverse direction of 12–13 kcal/mol from D1) are shown (Figure 3,

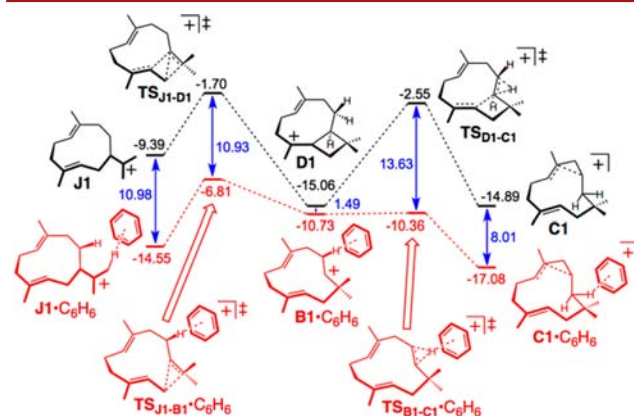


Figure 3. Potential energy surface for rearrangement of carbocation J1 to carbocation C1. Energies (kcal/mol) are relative to that of the farnesyl cation in a productive conformation for cyclization (A1 in Figure 2; black pathway) and the corresponding farnesyl cation + C₆H₆ complex (A1-C₆H₆ in Figure 4; red pathway), all computed with M06-2X/6-31+G(d,p)+ZPE. Predicted gas phase binding energies (differences between the energy of the complexes along the red pathway and the carbocations along the black pathway + benzene; gas phase; all are favorable) are shown in blue.

black; for results from other levels of theory and details on the remainder of the reaction coordinate, see Supporting Information). The mechanism found differs from that implied in Scheme 1 in that initial cyclization leads to a carbocation with a 10-membered ring that expands to a humulyl cation (C1) by way of an intermediate (D1). While a barrier of 13 kcal/mol can be

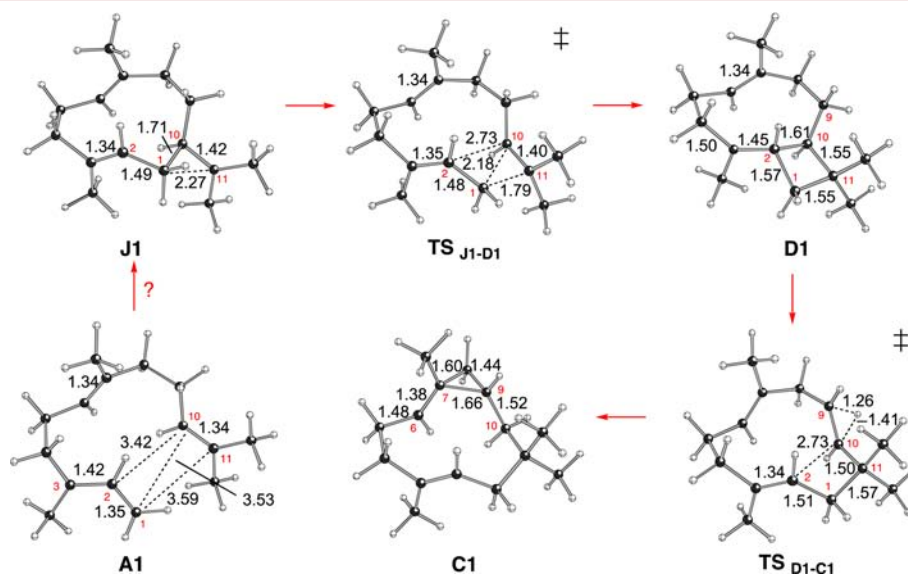


Figure 2. Computed structures of carbocation minima and transition state structures (M06-2X/6-31+G(d,p); distances in Å). We were unable to locate a transition state structure connecting farnesyl cation A1 and J1.

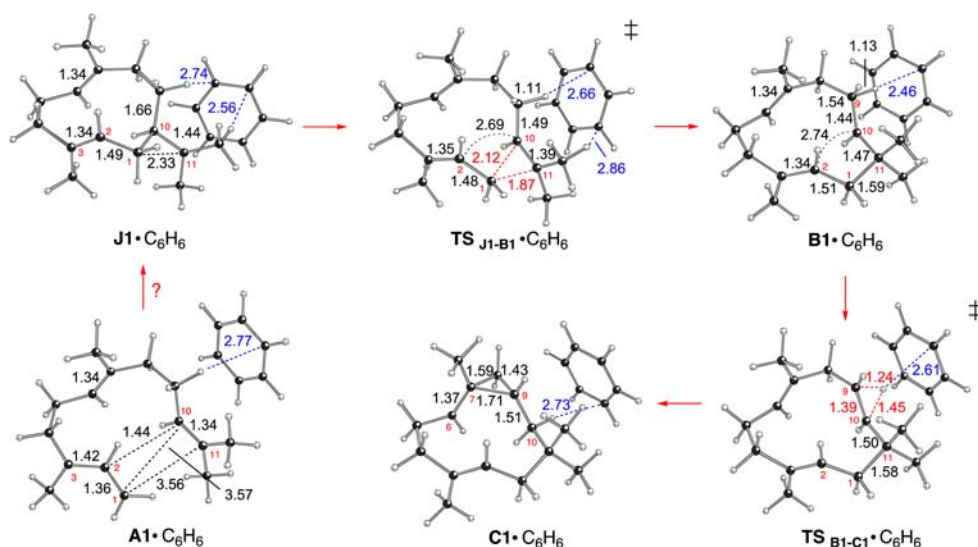


Figure 4. Computed benzene complexes of carbocations and transition state structures from Figure 2 (M06-2X/6-31+G(d,p); distances in Å). We were unable to locate a transition state structure connecting A1•C₆H₆ and J1•C₆H₆.

overcome at biologically relevant temperatures, barriers of this size are uncommon for terpene-forming carbocation reactions.³ Reducing the depth of this minimum would reduce the lifetime of carbocation **D1**, reducing the likelihood of its diversion to byproducts. Note that formation of **D1** is predicted to involve a concerted but asynchronous combination of 1,2-alkyl shifting and carbocation–alkene cyclization events, while further reaction of **D1** is predicted to involve a concerted but asynchronous combination of ring-opening and 1,2-hydride shifting events.^{3,19} Thus, the deep minimum on this reaction coordinate involves a “temporary cyclization”, related to the “temporary alkyl shift” described previously along one pathway to trichodiene⁶ and the temporary formation of a cyclobutane en route to pentalenene, another sesquiterpene.^{5a}

Complexation of the carbocations shown in Figure 2 by benzene, a simple model of the aromatic side chains that are regularly found in terpene synthase active sites (e.g., Phe, Tyr, Trp),²⁰ in the orientation shown in Figure 3 (red pathway) and Figure 4 altered the reaction coordinate dramatically. In the presence of benzene, there is no deep minimum. The reverse barrier is reduced to approximately 4 kcal/mol, and the forward barrier is reduced to a few tenths of a kcal/mol; essentially, the conversion of **J1** to **C1** is converted from a 2-step process with a deep intermediate to a process that is essentially (although not technically) concerted but very asynchronous. In addition, the temporary cyclization no longer occurs (note the C2–C10 distances in Figure 4).

Why is such a drastic change to the potential energy surface observed? It appears that this change reflects a tension between internal and external stabilization of carbocations along the reaction coordinate. For the benzene-free reaction, delocalization (of electrons and positive charge) occurs *within* the carbocations (Figure 2). For example, formation of a σ -bond and tertiary carbocation to form carbocation **D1** allows secondary carbocation **B1** (Figure 4) to be avoided.³ However, this shift of electron density within the carbocation leads directly to the deep minimum. In the presence of a benzene molecule, the secondary carbocation is stabilized through *external* C–H $\cdots\pi$ interactions that increase the strength of hyperconjugation between the C–H bond and the secondary carbocation center.^{10,21} As a result, **B1** does not collapse directly to **D1**.

The energy of free **D1** + free benzene is only 1.5 kcal/mol higher than that of the **B1** + benzene complex (Figure 3, blue), suggesting that the internal and external sources of stabilization just described have similar magnitudes. Note also that the following transition state structure is predicted to bind more strongly to benzene than any of the other stationary points in Figure 4 and that the associated barrier forward becomes negligible upon benzene complexation. Overall, the magnitude of binding to benzene is counterbalanced by loss of particular types of internal carbocation stabilization, allowing for differences in binding energies that result in changes to the relative energies of carbocations along the reaction coordinate. In the case described here, these changes convert a reaction coordinate with a deep minimum into one with a minimum so shallow as to have essentially no forward barrier, a scenario that promotes product formation

The results described here show that a deep minimum can be eradicated by simple complexation of a carbocation to the π -face of an aromatic, in the absence of a wholesale change of mechanism⁶ or a nonstatistical dynamic effect.⁴ For this scenario to occur, the carbocation in question must bind in a specific orientation in a terpene synthase active site that allows for selective binding interactions that promote product formation; we see no reason why an enzyme cannot accomplish such a feat. This strategy, among others, is now being applied to terpene synthase design and may find use in the design of other types of catalysts, both biological and synthetic.

■ ASSOCIATED CONTENT

Supporting Information

The Supporting Information is available free of charge on the ACS Publications website at DOI: 10.1021/acs.orglett.5b02740.

Coordinates and energies for all computed structures and additional computational data (PDF)

■ AUTHOR INFORMATION

Corresponding Author

*E-mail: djtantillo@ucdavis.edu.

Notes

The authors declare no competing financial interest.

ACKNOWLEDGMENTS

We gratefully acknowledge support from UC Davis and the National Science Foundation (CHE-0957416, CHE-1361807, and CHE030089 for supercomputing resources).

REFERENCES

- (1) Examples: (a) Sun, L.; Song, K.; Hase, W. L. *Science* **2002**, *296*, 875–878. (b) Kozuch, S.; Shaik, S. *Acc. Chem. Res.* **2011**, *44*, 101–110. (c) González-Lafont, A.; Moreno, M.; Lluch, J. M. *J. Am. Chem. Soc.* **2004**, *126*, 13089–13094. (d) Bond, P. J.; Wee, C. L.; Sansom, M. S. P. *Biochemistry* **2008**, *47*, 11321–11331.
- (2) (a) Miklis, P. C.; Ditchfeld, R.; Spencer, T. A. *J. Am. Chem. Soc.* **1998**, *120*, 10482–10489. (b) Heidrich, D. *Angew. Chem., Int. Ed.* **2002**, *41*, 3208–3210. (c) Filippi, A.; Roselli, G.; Renzi, G.; Grandinetti, F.; Speranza, M. *Chem. - Eur. J.* **2003**, *9*, 2072–2078. (d) Dougherty, D. A. *Science* **1996**, *271*, 163–168. (e) Farcasiu, D.; Hâncu, D. *J. Phys. Chem. A* **1997**, *101*, 8695–8700. (f) Kolboe, S. J. *J. Phys. Chem. A* **2011**, *115*, 3106–3115. (g) Kolboe, S. J. *J. Phys. Chem. A* **2012**, *116*, 3710–3716.
- (3) (a) Tantillo, D. J. *Nat. Prod. Rep.* **2011**, *28*, 1035–1053. (b) Tantillo, D. J. *Chem. Soc. Rev.* **2010**, *39*, 2847–2854. (c) Hong, Y. J.; Tantillo, D. J. *Chem. Soc. Rev.* **2014**, *43*, 5042–5050.
- (4) Pemberton, R. P.; Hong, Y. J.; Tantillo, D. J. *Pure Appl. Chem.* **2013**, *85*, 1949–1957.
- (5) (a) Zu, L.; Xu, M.; Lodewyk, M. W.; Cane, D. E.; Peters, R. J.; Tantillo, D. J. *J. Am. Chem. Soc.* **2012**, *134*, 11369–11371. (b) Jackson, A. J.; Hershey, D. M.; Chesnut, T.; Xu, M.; Peters, R. J. *Phytochemistry* **2014**, *103*, 13–21.
- (6) (a) Hong, Y. J.; Tantillo, D. J. *J. Am. Chem. Soc.* **2014**, *136*, 2450–2463. (b) Hong, Y. J.; Tantillo, D. J. *Org. Lett.* **2006**, *8*, 4601–4604. (c) Dickschat, J. S.; Brock, N. L.; Citron, C. A.; Tudzynski, B. *ChemBioChem* **2011**, *12*, 2088–2095.
- (7) (a) Christianson, D. W. *Curr. Opin. Chem. Biol.* **2008**, *12*, 141–150. (b) Davis, E. M.; Croteau, R. *Top. Curr. Chem.* **2000**, *209*, 53–95. (c) Cane, D. E. *Compr. Nat. Prod. Chem.* **1999**, *2*, 155–200. (d) Cane, D. E. *Chem. Rev.* **1990**, *90*, 1089–1103.
- (8) (a) Carpenter, B. K. *Acc. Chem. Res.* **1992**, *25*, 520. (b) Carpenter, B. K. *J. Phys. Org. Chem.* **2003**, *16*, 858. (c) Carpenter, B. K. *Annu. Rev. Phys. Chem.* **2005**, *56*, 57.
- (9) Ammal, S. C.; Yamataka, H.; Aida, M.; Dupuis, M. *Science* **2003**, *299*, 1555–1557.
- (10) Hong, Y. J.; Tantillo, D. J. *Chem. Sci.* **2013**, *4*, 2512–2518.
- (11) Jenson, C.; Jorgensen, W. L. *J. Am. Chem. Soc.* **1997**, *119*, 10846–10854.
- (12) Pemberton, R. P.; Tantillo, D. J. *Chem. Sci.* **2014**, *5*, 3301–3308.
- (13) Trefolane A was isolated from an edible fungus, the basidiomycete *Tremella foliacea*, by Liu et al.: Ding, J.-H.; Feng, T.; Li, Z.-H.; Yang, X.-Y.; Guo, H.; Yin, X.; Wang, G.-Q.; Liu, J.-K. *Org. Lett.* **2012**, *14*, 4976–4978.
- (14) Chiba, R.; Minami, A.; Gomi, K.; Oikawa, H. *Org. Lett.* **2013**, *15*, 594–597.
- (15) (a) For the other cases examined, no significant effect on well depth was found. (b) This is part 17 in our series on sesquiterpene-forming carbocation reactions. For part 16, see: Ortega, D. E.; Nguyen, Q. N. N.; Tantillo, D. J.; Toro-Labbe, A., submitted.
- (16) Selected examples: (a) Li, R.; Chou, K. W.; Himmelberger, J. A.; Litwin, K. M.; Harris, G. G.; Cane, D. E.; Christianson, D. W. *Biochemistry* **2014**, *53*, 1155–1168. (b) Ito, R.; Hashimoto, I.; Masukawa, Y.; Hoshino, T. *Chem. - Eur. J.* **2013**, *19*, 17150–17158. (c) Faraldos, J. A.; Antonczak, A. K.; González, V.; Fullerton, R.; Tippmann, E. M.; Allemann, R. K. *J. Am. Chem. Soc.* **2011**, *133*, 13906–13909. (d) Morikubo, N.; Fukada, Y.; Ohtake, K.; Shinya, N.; Kiga, D.; Sakamoto, K.; Asanuma, M.; Hirota, H.; Yokoyama, S.; Hoshino, T. *J. Am. Chem. Soc.* **2006**, *128*, 13184–13194.
- (17) (a) Chen, N.; Wang, S.; Smentek, L.; Hess, B. A., Jr.; Wu, R. *Angew. Chem., Int. Ed.* **2015**, *54*, 8693–8696. (b) Pemberton, R. P.; Ho, K. C.; Tantillo, D. J. *Chem. Sci.* **2015**, *6*, 2347–2353. (c) Tian, B.; Wallrapp, F. H.; Holiday, G. L.; Chow, J.-Y.; Babbitt, P. C.; Poulter, C. D.; Jacobson, M. P. *PLoS Comput. Biol.* **2014**, *10*, e1003874. (d) Major, D. T.; Weitman, M. *J. Am. Chem. Soc.* **2012**, *134*, 19454–19462. (e) Weitman, M.; Major, D. T. *J. Am. Chem. Soc.* **2010**, *132*, 6349–6360. (f) Rajamani, R.; Gao, J. *J. Am. Chem. Soc.* **2003**, *125*, 12768–12781.
- (18) All structures were optimized using Gaussian09 (Frisch, M. J.; et al. *Gaussian09*, revision B.01; Gaussian, Inc.: Pittsburgh, PA, 2010 (see [Supporting Information](#) for full reference)) using B3LYP/6-31+G(d,p) (Becke, A. D. *J. Chem. Phys.* **1993**, *98*, 5648–5652. Becke, A. D. *J. Chem. Phys.* **1993**, *98*, 1372–1377. Lee, C.; Yang, W.; Parr, R. G. *Phys. Rev. B: Condens. Matter Mater. Phys.* **1988**, *37*, 785–789. Stephens, P. J.; Devlin, F. J.; Chabalowski, C. F.; Frisch, M. J. *J. Phys. Chem.* **1994**, *98*, 11623–11627) and M06-2X/6-31+G(d,p) (Zhao, Y.; Truhlar, D. *Theor. Chem. Acc.* **2008**, *120*, 215–241). Single point energies on B3LYP/6-31+G(d,p) geometries were also computed with mPW1PW91/6-31+G(d,p) (Matsuda, S. P. T.; Wilson, W. K.; Xiong, Q. *Org. Biomol. Chem.* **2006**, *4*, 530–543) and MPWB1K/6-31+G(d,p) (Zhao, Y.; Truhlar, D. G. *J. Phys. Chem. A* **2004**, *108*, 6908–6918. Zheng, J.; Zhao, Y.; Truhlar, D. G. *J. Chem. Theory Comput.* **2007**, *3*, 569–582). The methods involving B3LYP geometry optimization have been applied previously to a variety of terpene-forming carbocation reactions.³ M06-2X/6-31+G(d,p) calculations, often employed when one worries about the effects of dispersion, have been applied previously to carbocation–benzene complexes;¹⁰ they were shown to predict binding energies larger than those predicted with B3LYP (and some range-separated functionals) but smaller than those predicted by, for example, ω B97X-D (basis set superposition errors [BSSE] for all methods were predicted to be ≤ 0.51 kcal/mol). M06-2X/6-31+G(d,p) results are discussed in the text (binding energies have not been corrected for BSSE), but results obtained with B3LYP/6-31+G(d,p), mPW1PW91/6-31+G(d,p)//B3LYP/6-31+G(d,p), and MPWB1K/6-31+G(d,p)//B3LYP/6-31+G(d,p) can be found in the [Supporting Information](#). Results from these levels of theory agree in most respects, differing primarily in that carbocation J and the farnesyl cation (with cation–alkene distances > 3.4 Å) are predicted to be separate minima with M06-2X/6-31+G(d,p), while a single minimum corresponding to a farnesyl cation with a tight cation–alkene interaction (distances < 2.8 Å) is found with B3LYP/6-31+G(d,p). Reverse and forward barriers flanking D for levels where B3LYP/6-31+G(d,p) optimizations were used ranged from 17–20 and 11–12 kcal/mol, respectively. Structural images were produced using Ball & Stick (Müller, N.; Falk, A.; Gsaller, G. *Ball & Stick*, V.4.0a12, molecular graphics application for MacOS computers; Johannes Kepler University: Linz, Austria, 2004). Carbocations are named using capital letters followed by numbers that refer to particular conformations (see [Supporting Information](#) for data on conformations not discussed in the text).
- (19) (a) Tantillo, D. J. *J. Phys. Org. Chem.* **2008**, *21*, 561–570. (b) Williams, A. *Concerted Organic and Bio-Organic Mechanisms*; CRC Press: Boca Raton, FL, 2000. (c) Hess, J. B. A. *J. Am. Chem. Soc.* **2002**, *124*, 10286–10287.
- (20) Christianson, D. W. *Chem. Rev.* **2006**, *106*, 3412–3442.
- (21) This hyperconjugation increases the partial positive charge on the H, thereby increasing favorable electrostatic attraction to the π -face of benzene; see ref 10.